

DNA-Tile-Directed Self-Assembly of Quantum Dots into Two-Dimensional Nanopatterns**

Jaswinder Sharma, Yonggang Ke, Chenxiang Lin, Rahul Chhabra, Qiangbin Wang, Jeanette Nangreave, Yan Liu,* and Hao Yan*

Organizing nanoparticles (NPs) into rationally designed ensemble structures is of great scientific interest because architecturally defined collective properties from multiple NPs could lead to applications such as photonic antennas and controlled plasmonic interactions.^[1] Recently, structural DNA nanotechnology has opened up new perspectives for the directed self-assembly of NPs^[2] and other molecular species^[3] into patterned nanostructures by taking advantage of the progress in the design and construction of artificial nanostructures with complex geometry or patterns through DNA self-assembly.^[4] Among these new techniques, the success of using DNA-tile-based nanostructures to organize NPs has been limited to only metallic gold NPs. To our knowledge, there has been no report demonstrating DNA-tile-directed self-assembly of semiconducting NPs (quantum dots, QDs) into rationally designed architectures; this may, in part, be due to the significantly different surface properties of QDs and gold NPs. The difficulty of making QDs compatible with DNA-tile-based nanostructures has prohibited many interesting studies of multicomponent NP photonic systems, for example, distance-dependent plasmonic quenching or enhancement between metallic NPs and QDs. Herein, we report a strategy for the use of two-dimensional DNA-tile arrays to direct the assembly of streptavidin-conjugated CdSe/ZnS core/shell QDs into well-defined periodic patterns. We anticipate that this first example of DNA-tile-based QD assembly will pave the way for the control of more sophisticated nanopatterns of QDs and beyond.

The strategy and schematic process of the DNA-tile-directed QD assembly is illustrated in Figure 1. We used a set of four double-crossover (DX) molecules, named the ABCD-tile system,^[5] as scaffolds for the QD assembly. Each different DX tile (DX-A, DX-B, DX-C, and DX-D) is shown by a different color in Figure 1. The A tile contains a short DNA

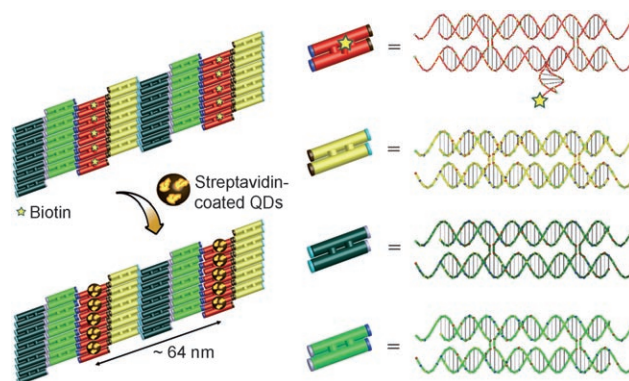


Figure 1. Process of DNA-tile-directed self-assembly of QD arrays.

stem protruding out of the tile plane that carries a biotin group (illustrated as a yellow star) at the end (see the Supporting Information for sequence details). Upon self-assembly, the four-tile system gives 2D arrays displaying parallel lines of biotin groups, with a periodic distance of approximately 64 nm between two neighboring biotin lines and a distance between two biotins within the line of about 4–5 nm. After addition of streptavidin-coated CdSe/ZnS QDs (Invitrogen; Qdot 545 ITK streptavidin conjugate, STV-QD) to the DNA array, the streptavidin molecules (illustrated as yellow blocks) specifically bind to the biotin groups so that the QDs (illustrated as black balls) will be organized onto the DX-tile arrays (see the Supporting Information for detailed methods).

The AFM images and cross-section profiles shown in Figure 2 clearly demonstrate that the STV-QDs bind specifically to the DX array and are organized into periodical stripes of QD arrays with the designed distances between the parallel lines. Due to the short stem on the A tile carrying the biotin group, the patterned 2D array of the ABCD-tile system alone (Figure 2, left image and blue trace) shows a small height change of approximately 0.5 nm across the line of the biotin groups. When the STV-QDs bind to the DX array (Figure 2, middle image and green trace), the average height across the biotin sites increases to about 9 nm. A control experiment with addition of streptavidin to the same type of biotin-modified DX array shows a height change of only approximately 2 nm (Figure 2, right image and red trace). The height change resulting from the STV-QD binding is significantly higher than that of the streptavidin binding to the array and the line widths are also much greater because of the much larger sizes of the STV-QDs (estimated diameter including the surface polymer and protein coating ≈ 10 nm) compared to those of the protein molecules alone (≈ 2 –3 nm).

[*] J. Sharma, Y. Ke, C. Lin, R. Chhabra, Dr. Q. Wang, J. Nangreave, Prof. Dr. Y. Liu, Prof. Dr. H. Yan
Department of Chemistry & The Biodesign Institute
Arizona State University
Tempe, AZ 85287 (USA)
Fax: (+1) 480-727-2378
E-mail: yan_liu@asu.edu
hao.yan@asu.edu

[**] This research was supported by grants from the National Science Foundation, National Institutes of Health, Air Force Office of Scientific Research, and Office of Naval Research, by grants from Arizona State University (ASU) to H.Y., and by faculty start-up funds from ASU to Y.L.

Supporting information for this article is available on the WWW under <http://dx.doi.org/10.1002/anie.200801485>.

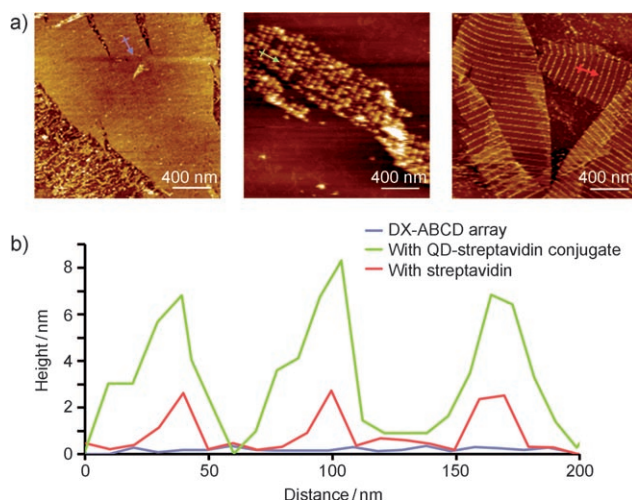


Figure 2. a) AFM images of the DX-ABCD array alone with each A tile bearing a biotin (left), the biotinylated DX-ABCD array incubated with STV-QD conjugate (middle), and the same array incubated with streptavidin only (right). b) Cross-section analysis of the AFM images. Each trace corresponds to the same colored arrow in (a).

TEM imaging further reveals the patterning of the QD arrays templated by DX tiles. The TEM images shown in Figure 3 represent the periodic alignment of QDs into parallel stripes with a measured periodicity of about 64 nm between the lines, which matches well with the designed parameters. The diameter of each individual QD particle is measured as approximately 4 nm, which corresponds to the size of CdSe/ZnS QDs with green emission. The protein and polymer coatings on the surface of the QDs are not visible due to low electron density and, thus, low contrast in the TEM image. It is notable that the QDs within each stripe sometimes shift

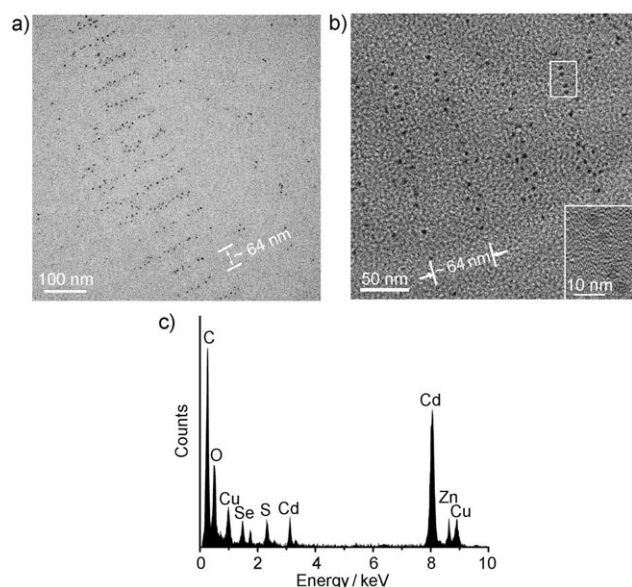


Figure 3. a) TEM image of the periodic pattern of the organized QD arrays. b) High-resolution TEM image (with a close-up inset) that reveals the crystalline structure of the QDs. c) EDX spectrum that verifies the composition of the CdSe/ZnS QDs.

slightly out of the line; this may be due to the orientational flexibility of the short protruding DNA stems bearing the biotin group and the tendency of neighboring QDs to avoid steric crowding. The center-to-center distance between QDs within the same line measures from 7 to 15 nm, which is larger than the distance between neighboring biotin groups (4–5 nm) in the DX array. This can be explained by the large size of the protein-coated QDs causing steric hindrance within the line. The multiple streptavidin molecules conjugated on each QD and the multivalency of the streptavidin–biotin binding may also contribute to this effect. It is possible that multiple streptavidin molecules on a single QD may be in orientations that allow for the binding of two or three neighboring biotin groups in the same line. By taking the size of the QD with the protein and polymer coating on the surface into account, this 7–15 nm distance is close to the highest possible packing density of the protein-coated QDs in the line. More TEM and AFM images of larger sample areas, demonstrating the fidelity of the successful assembly of the STV-QDs by using the DNA-tile scaffolds, are included in the Supporting Information. High-resolution TEM images (insert in Figure 3 b) clearly reveal the crystalline structure of the QDs, and the energy-dispersive X-ray (EDX; Figure 3 c) data support the idea that the NPs in the image are composed of CdSe/ZnS.

In addition to AFM and TEM imaging, we further used laser fluorescence imaging and photobleaching experiments to demonstrate that the QDs were assembled onto the DX array. In this experiment, a DNA strand in the B tile of the DX array was modified with an organic fluorophore with red emission, namely cyanine 5 (Cy5; $\lambda_{\text{em}} = 648 \text{ nm}$). The DX arrays carrying both Cy5 and STV-QD with green emission ($\lambda_{\text{em}} = 545 \text{ nm}$) were imaged by fluorescence imaging (Figure 4 a), which revealed the colocalization of red Cy5 and green QDs on the DNA array (see the superimposed fluorescence image in Figure 4 a). It is well known that QDs have higher photostability than organic fluorophores. A rectangular shaped region of $11 \times 15 \mu\text{m}^2$ was selected from the imaged area to be photobleached (Figure 4 b). This region was constantly irradiated by a focused 405 nm laser beam at a power of 0.9 mW for 81 s. Images were taken with 9 s intervals during the photobleaching process by using the same sequential scanning setup. The change in the relative intensity of the red and green fluorescence in the bleached region is plotted in Figure 4 b. It is clear that the organic fluorophore was photobleached with a 90% drop in intensity within 30 s, whereas the emission intensity of the green QDs still persists after 80 s. This experiment further indicates that the QDs are successfully organized onto the DNA-tile arrays.

In summary, we have constructed well-aligned two-dimensional arrays of QDs with controlled periodicity by coupling DNA self-assembly with the use of streptavidin-coated QDs. As an elegant bottom-up method, DNA self-assembly has an inherent advantage in generating programmable nanostructures with rationally designed functionality and nanometer precision in addressability. Our work demonstrates the capability for directing QDs into designer nanoarchitectures; this opens up opportunities to construct discrete nanostructures of multicomponent NP systems for energy and biosensing applications. It is worth pointing out

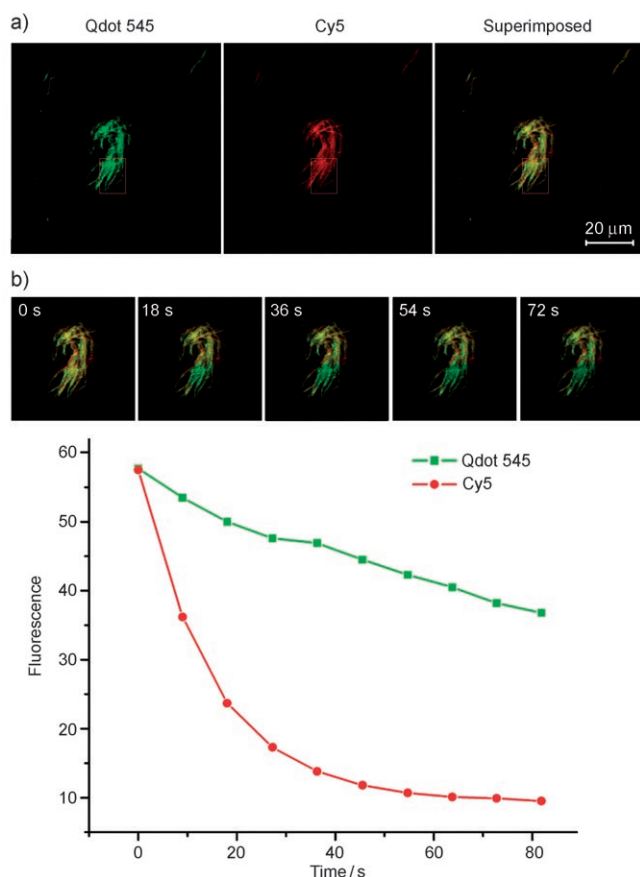


Figure 4. a) Confocal fluorescence microscopy images and b) photobleaching on the DNA arrays. Scale bar: 20 μm .

that both the surface and bioconjugation chemistry of QDs are much more complicated than those of gold nanoparticles; this led us to optimize many important experimental parameters to achieve successful QD assembly on the DNA-tile arrays (see the Supporting Information for further comments). We acknowledge that more robust bioconjugation chemistry on the QDs to obtain DNA-sequence-coded QDs (for example, it would be desirable to have a discrete number of DNA oligomers displayed on the QD surface) is needed for

sequence-addressable organization of the QDs into more sophisticated architectures. By combining QD-assembly strategies with the previous success of metallic-NP organization, we expect that many new properties of well-controlled multicomponent nanophotonic structures will be revealed. Indeed, the organizational power of structural DNA nanotechnology is so far only at the horizon.

Received: March 28, 2008

Published online: June 4, 2008

Keywords: DNA · nanostructures · quantum dots · self-assembly

- [1] S. L. Westcott, S. J. Oldenburg, T. R. Lee, N. J. Halas, *Chem. Phys. Lett.* **1999**, *300*, 651–655.
- [2] a) J. D. Le, Y. Pinto, N. C. Seeman, K. Musier-Forsyth, T. A. Taton, R. A. Kiehl, *Nano Lett.* **2004**, *4*, 2343–2347; b) J. Zhang, Y. Liu, Y. Ke, H. Yan, *Nano Lett.* **2006**, *6*, 248–251; c) J. Sharma, R. Chhabra, Y. Liu, Y. Ke, H. Yan, *Angew. Chem.* **2006**, *118*, 744–749; *Angew. Chem. Int. Ed.* **2006**, *45*, 730–735; d) Z. Deng, Y. Tian, S.-H. Lee, A. E. Ribbe, C. Mao, *Angew. Chem.* **2005**, *117*, 3648–3651; *Angew. Chem. Int. Ed.* **2005**, *44*, 3582–3585; e) H. Li, S. H. Park, J. H. Reif, T. H. LaBean, H. Yan, *J. Am. Chem. Soc.* **2004**, *126*, 418–419; f) J. H. Lee, D. P. Wernette, M. V. Yigit, J. Liu, Z. Wang, Y. Lu, *Angew. Chem.* **2007**, *119*, 9164–9168; *Angew. Chem. Int. Ed.* **2007**, *46*, 9006–9010; g) F. Aldaye, H. F. Sleiman, *Angew. Chem.* **2006**, *118*, 2262–2267; *Angew. Chem. Int. Ed.* **2006**, *45*, 2204–2209; h) F. Aldaye, H. F. Sleiman, *J. Am. Chem. Soc.* **2007**, *129*, 4130–4131.
- [3] a) H. Yan, S. H. Park, G. Finkelstein, J. H. Reif, T. H. LaBean, *Science* **2003**, *301*, 1882–1884; b) R. Chhabra, J. Sharma, Y. Ke, Y. Liu, S. Rinker, S. Lindsay, H. Yan, *J. Am. Chem. Soc.* **2007**, *129*, 10304–10305; c) B. A. R. Williams, K. Lund, Y. Liu, H. Yan, J. C. Chaput, *Angew. Chem.* **2007**, *119*, 3111–3114; *Angew. Chem. Int. Ed.* **2007**, *46*, 3051–3054; d) Y. He, Y. Tian, A. E. Ribbe, C. Mao, *J. Am. Chem. Soc.* **2006**, *128*, 12664–12665.
- [4] a) N. C. Seeman, *Nature* **2003**, *421*, 427–431; b) U. Feldkamp, C. M. Niemeyer, *Angew. Chem.* **2006**, *118*, 1888–1910; *Angew. Chem. Int. Ed.* **2006**, *45*, 1856–1876; c) P. W. K. Rothmund, *Nature* **2006**, *440*, 297–302; d) K. V. Gothelf, T. H. LaBean, *Org. Biomol. Chem.* **2005**, *3*, 4023–4037; e) C. Lin, Y. Liu, H. Yan, *ChemPhysChem* **2006**, *7*, 1641–1647.
- [5] F. Liu, R. Sha, N. C. Seeman, *J. Am. Chem. Soc.* **1999**, *121*, 917–922.